

Spinodals and the Temperature-Dependent Compressive Strength of Crystalline Poly(*p*-phenylene terephthalamide)

Daniel J. Lacks

Department of Chemical Engineering, Tulane University, New Orleans, Louisiana 70118

Received January 2, 2001; Revised Manuscript Received March 19, 2001

ABSTRACT: Molecular simulations are carried out to determine the spinodal of crystalline poly(*p*-phenylene terephthalamide) (PPTA) with respect to temperature and compressive axial stress. The simulations show that the temperature of the spinodal decreases with increasing compressive axial stress, and vice versa. This coupling of the effects of temperature and stress occurs because both increased temperature and compressive axial stress lead to axial contraction in the crystal, and the spinodal corresponds to an Euler buckling instability that occurs when the axial lattice parameter falls below a critical value. The simulation results for the spinodal are very similar to the experimental results for the temperature-dependent compressive strength of Kevlar fibers (which are composed of semicrystalline PPTA), suggesting that the compressive failure of Kevlar fibers arises from the spinodal of the PPTA crystal phase, rather than a defect-mediated mechanism.

I. Introduction

Polymer fibers, such as Kevlar, are widely used in composite materials due to their high specific stiffness and strength. The composite materials are often used in structural applications under external stresses and elevated temperatures, and so the temperature dependence of the fiber strength can have important consequences. The present paper addresses the temperature dependence of the compressive strength of poly(*p*-phenylene terephthalamide) (PPTA) crystals, which comprise Kevlar fibers.

This paper focuses on the possibility of a relationship between the compressive strength of Kevlar fibers and the spinodal of PPTA crystals. The spinodal represents the metastability limits of the crystal, which differs from the thermodynamic stability limits; the metastability limits are associated with the conditions for which a free energy minimum corresponding to the phase exists, while the thermodynamic stability limits are associated with the conditions for which this free energy minimum is the global minimum. The spinodal is likely to be more important than thermodynamic stability limits in regard to the mechanical properties of crystals because the long relaxation times in solids often hinder thermodynamic solid–solid transitions.

Previous continuum models¹ and molecular simulations² have shown that the strength of polymer crystals under axial compressive stress is limited by an Euler buckling instability, which represents the spinodal of the crystal with respect to applied axial stress. Alternatively, defect-mediated mechanisms may cause material failure before the spinodal is reached.³ Regarding the effects of temperature, molecular simulations of polyethylene crystals have shown that increased temperature leads to an entropically induced axial compressive stress that augments an applied axial compressive stress, causing the spinodal stress to decrease as the temperature increases (or, equivalently, the spinodal temperature to decrease as the applied stress increases).⁴ However, we are not aware of experimental results for polyethylene that allow an assessment of a relationship between the spinodal and the *temperature-dependent* compressive strength. The present paper

addresses this relationship in Kevlar fibers, for which such experimental data exist.⁵

II. Computational Methods

Molecular simulations are carried out to determine the range of temperature and applied axial stress for which there exists a minimum of the Gibbs free energy corresponding to $P2_1/n$ PPTA crystal phase. (The $P2_1/n$ PPTA crystal phase is the stable crystal phase under ordinary conditions.⁶) The boundary of this range is the spinodal of the crystal phase with respect to temperature and applied axial stress.

The simulation methods used here have been described in detail elsewhere^{7,8} and shown to give good results for the thermodynamic properties of PPTA⁷ and other polymers⁸ over a fairly wide temperature range. The Gibbs free energy is evaluated as the sum of the potential energy, stress–strain energy, and vibrational free energy and is a function of temperature, stress, and the lattice parameters of the crystal. (There are four lattice parameters for the $P2_1/n$ PPTA crystal structure: a , b , c , and an angle γ .) At fixed temperature and stress, the equilibrium crystal structure corresponds to the lattice parameters that minimize the Gibbs free energy. (Thus at equilibrium, the Gibbs free energy is a function of temperature and stress only.)

The potential energy is determined with the PCFF force field,⁹ and Ewald methods are used to sum the long-range Coulombic and dispersion interactions. The vibrational free energy is calculated with quasi-harmonic lattice dynamics, which uses the quantum mechanical harmonic oscillator partition function with the harmonic vibrational frequencies of the crystal as input.¹⁰ Fourier space (Brillouin zone) methods are used to include vibrational modes of all wavelengths.¹⁰ The vibrational frequencies are determined by first varying the atomic positions to minimize the potential energy (at fixed lattice parameters), then calculating the dynamical matrix (which is related to the matrix of second derivatives of the potential energy) for each Fourier space wavevector, and then diagonalizing the dynamical matrix; the vibrational frequencies are obtained from the eigenvalues of the dynamical matrix. The vibra-

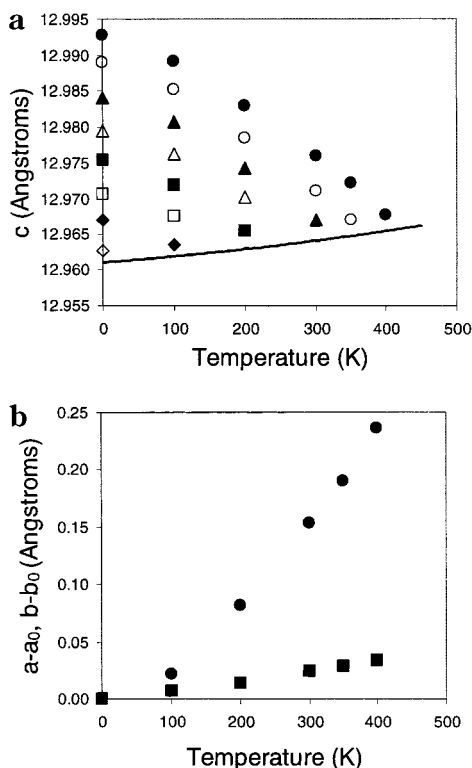


Figure 1. Minimum free energy structures of the PPTA crystal. (a) Results for the *c* lattice parameter as a function of temperature and applied axial compressive stress. Filled circles, 0 MPa; open circles, 100 MPa; filled squares, 200 MPa; open squares, 300 MPa; filled triangles, 400 MPa; open triangles, 500 MPa; filled diamonds, 600 MPa; open diamonds, 700 MPa. (b) Results for the changes in the *a* and *b* lattice parameters as a function of temperature. Circles: *a* - *a*₀ (*a*₀ = 8.06 Å). Squares: *b* - *b*₀ (*b*₀ = 5.14 Å). The changes in the *a* and *b* lattice parameters with applied axial stress are very small and not shown.

tional free energy is integrated over the Brillouin zone using a piecewise Gauss–Legendre integration scheme with 100 integration points that is designed to sample a wavevector $\mathbf{k} = (0,0,\epsilon)$ where ϵ is very small. (As discussed in the Results section, the spinodal occurs by an instability in this region of the Brillouin zone.)

The procedure to determine whether Gibbs free energy minimum exists for the crystal structure at a given temperature and stress involves varying the lattice parameters to minimize the free energy, using the experimental lattice parameters as a starting point. This procedure converges to a stable structure if the free energy minimum exists, but the procedure moves the system to an unstable structure (characterized by imaginary vibrational frequencies) if the free energy minimum does not exist.

III. Results

The results for the minimum free energy structures of the PPTA crystal are shown in Figure 1 as a function of temperature and applied axial stress. Increased axial compressive stress obviously causes contraction along the chain axis, as well as a very small expansion perpendicular to the chain axis. Increased temperature causes expansion perpendicular to the chain axis, but contraction along the chain axis, in agreement with experiment.¹¹ The axial thermal contraction is driven by the increase in entropy associated with enhanced vibrations perpendicular to the chain axis as the chain

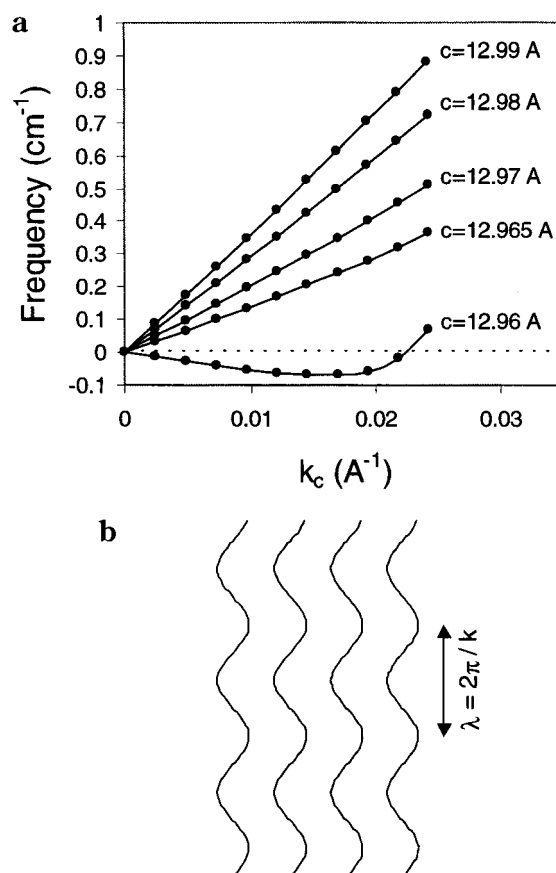


Figure 2. (a) Vibrational frequencies of the long-wavelength axial transverse acoustic modes. Imaginary frequencies are shown here as negative. (b) Schematic representation of the axial transverse acoustic modes

length decreases, as well as elastic coupling to the thermal expansion along the other directions.⁷ No stable structures exist below the line shown in Figure 1a.

The free energy minimum corresponding to the *P*₂₁/*n* PPTA crystal phase disappears when the axial lattice parameter decreases below a critical value (the line in Figure 1a). The decrease in the axial lattice parameter may be caused by either temperature or stress, or a combination of both. The reason for the disappearance of the free energy minimum becomes evident when the frequencies of the axial transverse acoustic modes (TAMs) are examined; the frequencies of these modes, shown in Figure 2, decrease to zero as the axial lattice parameter is decreased. The decrease to zero of the TAM frequencies implies that a bifurcation in the potential energy landscape occurs with respect to the TAM displacements, which is shown schematically in Figure 3; after the bifurcation occurs, the crystal structure is no longer stable. This spinodal mechanism is equivalent to an Euler buckling instability. Since Euler buckling is inhibited by the interactions with neighboring polymer chains,¹ and thermal expansion causes the polymer chains to move further apart, the critical value of the axial lattice parameter necessary to cause Euler buckling increases slightly with increasing temperature, as shown in Figure 1a.

IV. Discussion

The results for the spinodal of the *P*₂₁/*n* PPTA crystal phase are summarized in Figure 4. The spinodal temperature decreases with increasing applied axial stress,

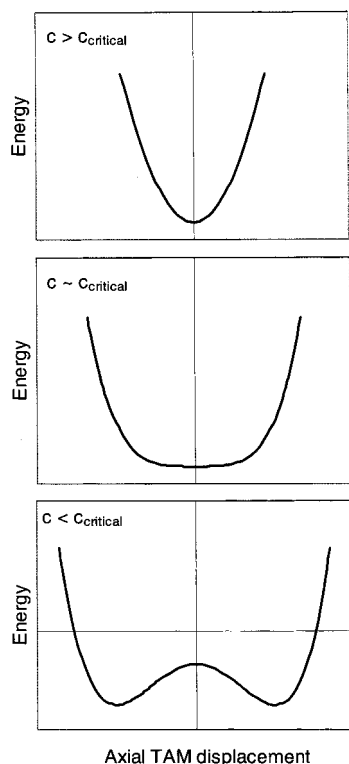


Figure 3. Schematic representation of the changes in the energy landscape underlying an Euler buckling instability (c is the axial lattice parameter).

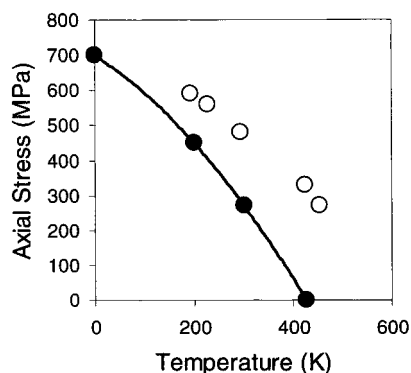


Figure 4. Filled circles: spinodal for PPTA crystallites from present simulations. Open circles: experimental compressive strength results for Kevlar 49 fibers, obtained from ref 5 as described in the text.

and vice versa. This result arises because both temperature and applied axial compressive stress lead to axial contraction in the crystal, and the spinodal occurs by an Euler buckling mechanism when the axial lattice parameter decreases below a critical value.

To assess the relevance of this spinodal, we compare it to experimental results for the temperature-dependent compressive strength of Kevlar fibers. Experimental results are available for a Kevlar 49/epoxy composite with 60% Kevlar by volume;⁵ results for the Kevlar fiber alone can be derived from the results for the composite under the assumptions that the Kevlar fibers and the epoxy matrix support an applied stress in parallel and that the stiffness of the fiber is much greater than that of the matrix. Under these assumptions, the compressive strength of the fiber is obtained as the compressive strength of the composite divided by the volume fraction of fiber.

As shown in Figure 4, the simulation results for the spinodal of the $P2_1/n$ PPTA crystal phase are very similar to the experimental results for the temperature-dependent compressive strength of Kevlar fibers. This similarity suggests that crossing the spinodal of the PPTA crystal phase, rather than a defect-mediated mechanism, causes the compressive failure of Kevlar fibers.

The spinodal has significance in regard to heating as well as compression. If the crystal is heated at low applied stresses, the spinodal temperature is above the melting temperature and will not be reached because melting (a thermodynamic transition) will occur first. However, as the applied stress becomes large enough, the spinodal temperature will decrease to a value below the melting temperature; in this case, heating the crystal above the spinodal temperature will trigger a transition to another solid structure.

The present simulations cannot determine the outcome of the spinodal instability, but only the point at which the spinodal occurs. Another crystal structure presumably becomes thermodynamically stable before the spinodal is reached (at temperatures below the melting temperature), but this thermodynamic transformation will be kinetically hindered, and so the result of the spinodal instability will likely be a disordered solid structure. In a semicrystalline material such as a Kevlar fiber, the stresses are not distributed uniformly, and the spinodal instability will occur first in only part of the material where the stress is concentrated; the distortions caused by the instability in a macroscopically localized region may relieve the stress for the rest of the material and give rise to shear bands as seen experimentally.

The choice of the simulation method is now addressed. A key concern is that the spinodal instability occurs by a large length scale mechanism. A small system size in a direct space simulation (e.g., molecular dynamics) inhibits this instability—more specifically, the critical stress for an Euler buckling instability $\approx A + B/(\text{system length})^2$ where A and B are constants.¹ The lattice dynamics approach is therefore used due to its efficiency in accounting for large length scale motions in Fourier space. A disadvantage of the lattice dynamics method is that there is likely to be significant quantitative error associated with the quasi-harmonic approximation near the stability limits. Results on simple systems show that the quasi-harmonic approximation leads to underestimates of the spinodal temperature of a crystal;¹² the deficiencies of the quasi-harmonic approximation may thus be what causes the spinodal curve from simulation to underestimate the compressive strength curve from experiment, as shown in Figure 4. (Of course, the approximate nature of the force fields could also lead to such errors.)

The present results for perfect infinite crystals are expected to be applicable to real PPTA fibers that have defects (such as chain ends). For PPTA fibers, the defects are concentrated in layers, with the defect layers separated by ~ 350 Å;¹³ this distance between defect layers defines an effective crystallite thickness. Since an effective crystallite thickness of ~ 350 Å is large enough for instabilities to occur at critical stresses close to the critical stresses in the infinite system size limit (e.g., see Figure 2), the present results should be applicable to real PPTA fibers.

V. Conclusions

Molecular simulations show that the spinodal of crystalline PPTA with respect to axial compressive stress and temperature corresponds to an Euler buckling instability. The simulation results for the spinodal of the $P2_1/n$ PPTA crystal phase are very similar to the experimental results for the temperature-dependent compressive strength of Kevlar fibers, which suggests that the compressive failure of Kevlar fibers is caused by crossing the spinodal of the PPTA crystal phase. Also, the spinodal temperature decreases to a value below the melting temperature as the applied stress becomes large enough, and we predict that under these conditions heating the crystal will trigger a transition to another solid structure when the temperature surpasses the spinodal temperature.

Acknowledgment. Funding for this project was provided by the National Science Foundation (Grants DMR-9624808 and DMR-0080191).

References and Notes

- (1) DeTeresa, S.; Porter, R.; Farris, R. J. *J. Mater. Sci.* **1985**, *20*, 1645–1659.
- (2) McGann, M. R.; Lacks, D. J. *Macromolecules* **1998**, *31*, 6356–6361.
- (3) Lacks, D. J. *J. Mater. Sci.* **1996**, *31*, 5885–5889.
- (4) Vlattas, C.; Galiotis, C. *Polymer* **1994**, *35*, 2335–2347.
- (5) McGann, M. R.; Lacks, D. J. *Phys. Rev. Lett.* **1999**, *82*, 952–955.
- (6) Wilfong, R. E.; Zimmerman, J. *J. Appl. Polym. Sci., Appl. Polym. Symp.* **1977**, *31*, 1–21.
- (7) Tadokoro, H. *Structure of Crystalline Polymers*; John Wiley and Sons: New York, 1979.
- (8) Lacks, D. J.; Rutledge, G. C. *Macromolecules* **1994**, *27*, 7197–7204.
- (9) Rutledge, G. C.; Lacks, D. J.; Martonak, R.; Binder, K. *J. Chem. Phys.* **1998**, *108*, 10274–10280.
- (10) PCFF Force field, from “Discover Software, version 2.3”; Biosym Technologies, San Diego, 1993.
- (11) Ashcroft, N. W.; Mermin, N. D. *Solid State Physics*; Saunders College Press: Philadelphia, 1976.
- (12) Ii, T.; Tashiro, K.; Kobayashi, M.; Tadakoro, H. *Macromolecules* **1987**, *20*, 347–351.
- (13) Klein, M. L.; Horton, G. K.; Feldman, J. L. *Phys. Rev.* **1969**, *184*, 969–978.
- (14) Panar, M.; Avakian, P.; Blume, R. C.; Gardner, K. H.; Gierke, T. D.; Yang, H. H. *J. Polym. Sci., Polym. Phys. Ed.* **1983**, *21*, 1955–1969.

MA0100044